Real-time condition monitoring of IGBT modules in PV inverter systems

Ui-Min Choi and Frede Blaabjerg
Center of Reliable Power Electronics (CORPE), Department of Energy Technology, Aalborg University, Aalborg, Denmark

Abstract

This paper proposes a new method for the real-time condition monitoring of IGBT modules in PV inverter system. The proposed method uses only one monitoring parameter, V_{CE_ON} and the wear-out failure modes of IGBT modules, bond-wire fatigue and solder joint fatigue can be distinguished by the V_{CE_ON} values at two measurement points. Thus, it is cost-effective compared with using one more monitoring parameter in order to separate failure modes. Furthermore, the proposed method does not require re-characterizations of IGBT modules as it is worn out. Experimental results verify the validity and feasibility of the proposed method.

1 Introduction

PV inverters are one of the most reliability-critical parts in PV systems [1]. The unscheduled maintenance events and costs by the subsystems have been investigated based on field experiences between 2001 and 2006 in a large utility-scale PV generation plant. The PV inverter covers 37 % of unscheduled maintenance events and make up 59 % of unscheduled maintenance costs. It can be seen from this result that the PV inverter is one of the important parts in respect to the reliability in the overall PV system and also to reduce the cost of operation [1].

Figure 1 shows the typical configuration of three-phase grid-connected PV inverter system which consists of DC/DC boost converter and DC/AC grid-connected inverter. Depending on the applications and power ratings, DC/DC converter is included or not [2].

The power devices are taking a large portion of the main failure causes of inverters and thus they are key components in respect to the reliability of PV inverter systems [3]. Among power devices, IGBT modules with wire-bonded packaging technology are most widely used in various applications [4] and thus it is worth to focus on condition monitoring of wire-bonded IGBT modules.

A real-time wear-out condition monitoring of IGBT modules with the determination of failure modes can allow proactive maintenance plans and also can help to avoid catastrophic failure of power converter systems. Further, it provides information for performing proactive control schemes such as load management, fault-tolerant control and thermal control [5]-[9].

It is well-known that bond-wire and solder joint fatigues are major failure mechanisms of wire-bonded IGBT modules [10] and an on-state collector-emitter voltage (V_{CE_ON}) is the key parameter for the detection of both failure modes [11]. However, when V_{CE_ON} is used for the condition monitoring, the interference of each failure mode on the other failure mode should be eliminated. For this, re-characterization of IGBT module is required [11] but this process is not applicable to real PV inverter systems and time-consuming even though it is possible.

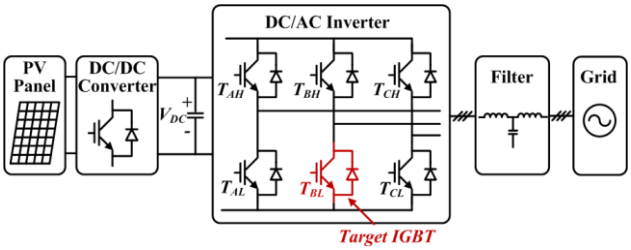

Figure 1 Configuration of three-phase grid-connected PV inverter system.

This paper proposes a new method for the monitoring of wear-out status of IGBT modules with the separation of two representative failure modes. It can be achieved by monitoring the two V_{CE_ON} values. Experimental results verify the validity and feasibility of the proposed method.

2 Real-time V_{CE_ON} and V_F measurement circuit

Figure 2 shows the real-time V_{CE_ON} and V_F measurement circuit based on a depletion mode MOSFET (M) for high side components. The drain of MOSFET is connected to the positive DC-link and collector of the IGBT. The source of MOSFET is connected to the op-amp through resistor (R) and a clamping circuit is also connected in parallel, where the magnitude of clamping voltage (V_{CC}), which is 5 V in this circuit, should be larger than that of V_{CE_ON} and V_F.

When T_H is turned on, the current I_M does not flow through M because the collector voltage $V_C = V_{CE\_ON} < V_{CC}$ and the input impedance of op-amp is high. Thus, $V_{GS} = 0$. Consequently, M is turned on since it has a negative threshold voltage and thus $V_{out\_H} = V_{CE\_ON}$. When V_C increases above V_{CC} as T_H is turned off, I_M starts to flow and makes a voltage drop in R. As I_M increases, V_{GS} becomes a negative value and then M is turned off when $V_{GS} < V_T$. Therefore, V_{CC} is measured at the output during this period [12].

ISBN 978-3-8007-4540-1

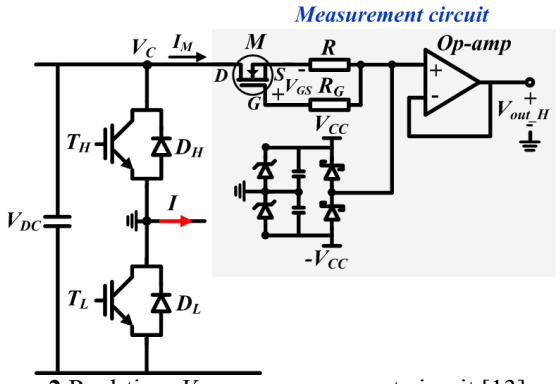

Figure 2 Real-time V_{CE_ON} measurement circuit [13].

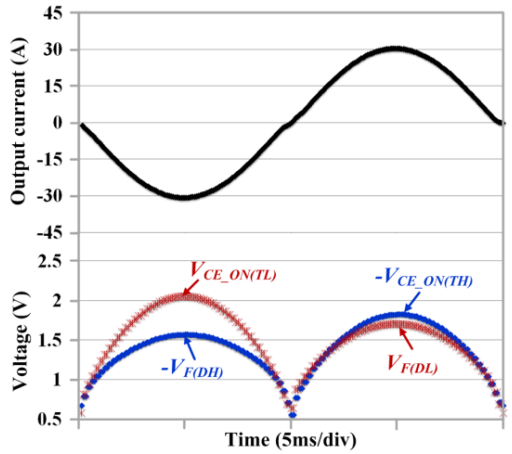

Figure 3 Measured V_{CE_ON} and V_F of IGBTs and diodes when the current is 30 A_{peak} and output frequency is 50 Hz.

Figure 3 shows the measured V_{CE_ON} and V_F of IGBTs and diodes by the real-time V_{CE_ON} and V_F measurement circuit when the current is 30 A_{peak} and the output frequency is 50 Hz.

3 Condition monitoring strategy with failure mode separation

3.1 Initial characterizations of IGBT modules

In this method, two V_{CE_ON} values at the intersection point of I-V characterization curves and at the peak of output current are used. In order to find the intersection point of I-V curves and to determine the failure modes by two V_{CE_ON}, two kinds of preliminary I-V characterizations of IGBT modules are required.

The first one is a conventional I-V characterization method. If an initial I-V charaterization is possible, the characterzation of IGBT modules can be perfromed by a simple switching sequence with real-time V_{CE_ON} measurement circuit as proposed in [13]. The intersection point and coressponding value ($V_{CE\_ON(int)}$) can be found from conventional I-V charaterization curves as shown in Figure 4(a).

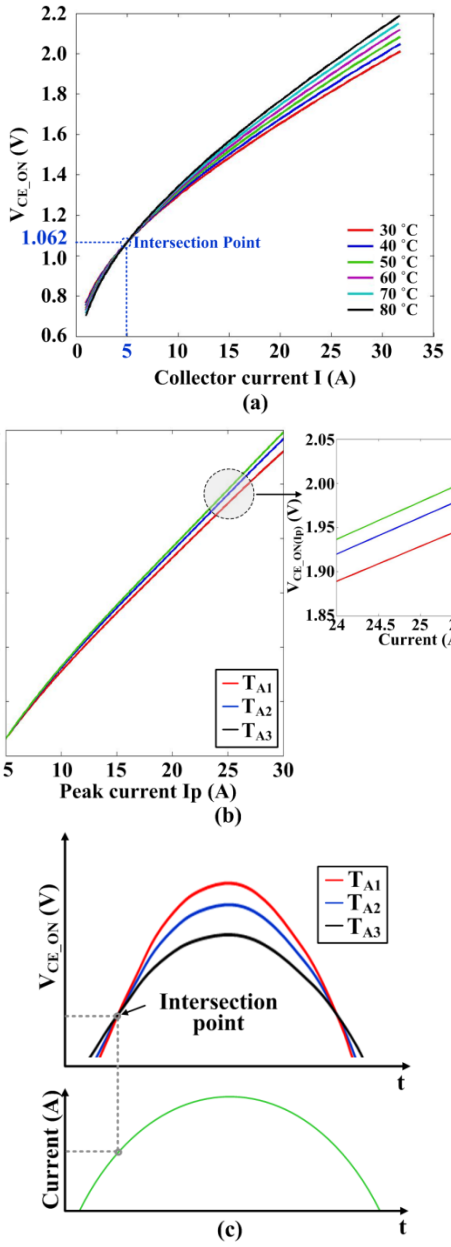

Figure 4 Characterization of IGBT modules ($T_{A1} > T_{A2} > T_{A3}$) (a) Conventional I-V characterization curves for $V_{CE\_ON(int)}$ (b) I-V characterization by output currents of an IGBT for $V_{CE\_ON(Ref\_Ip)}$. (c) V_{CE_ON} at the same output current under different T_As to find $V_{CE\_ON(int)}$ and $V_{CE\_ON(Ref\_Ip)}$.

This value is independent on temperature and therefore, the increase of electrical resistance (ΔR_{eq}) can be obtained from the variation of $V_{CE\_ON(int)}$ at intersection point ($\Delta V_{CE\_ON(int)}$).

The other I-V characterization is done by using sinusoidal currents in the operating range of the inverters under different temperatures, where V is V_{CE_ON} at peak current ($V_{CE\_ON(Ip)}$), I is the peak current (I_p) and the temperature is the measurable temperature outside of the IGBT module such as heat-sink temperature (T_H), case temperature (T_C) or ambient temperature (T_A) as shown in Figure 4(b). From this curves, the reference V_{CE_ON} at the

peak current ($V_{CE\_ON(Ref\_Ip)}$) can be obtained when I_p and T_A are known. This value is used for determining the failure mechanism. Further, K-factor, which is the dependency of $V_{CE\_ON(Ip)}$ on junction temperature (T_j) variation at a given I_p can be obtained indirectly.
However, in industrial applications, typically each module is not initially characterized. In this case, real-field data can be used for the two I-V characterizations, as mentioned above. It can be assumed that there is no visible degradation in the IGBT modules at the beginning of its installation (i.e first half year or several months). Therefore, the information for the charaterization of the IGBT modules can be obtained, when the inverter is operated in the real-field. Thanks to real-time V_{CE_ON} measurement circuit, V_{CE_ON} under the different ambient temperatures (T_A) at the same output current can be measured as shown in Figure 4(c) since typically, PV inverter measures T_A. V_{CE_ON} at differnt output currents under the different ambient temperatures (T_A) also can be used. From this, the intersection point and corresponding value ($V_{CE\_ON(int)}$) can be found. Further, the other I-V characterization curves with sinusoidal currents under different T_As can be obtained for $V_{CE\_ON(Ref\_Ip)}$.

3.2 Failure mode separation strategy

The variation of R_{eq} (ΔR_{eq}) due to bond-wire fatigue can be obtained by the increased value of V_{CE_ON} at the intersection point ($\Delta V_{CE\_ON(int)}$) as

$$\Delta R_{eq} = \Delta V_{CE\_ON(int)} / I_{int} \tag{1}$$

From the obtained ΔR_{eq}, the increment in V_{CE_ON} at I_p ($\Delta V_{CE\_ON(Ref\_Ip)}$) can be expected as

$$\Delta V_{CE\_ON(Ref\_Ip)} = \Delta R_{eq} \cdot I_p \tag{2}$$

Therefore, if the there is a variation in R_{eq} and the $V_{CE\_ON(Ip)}$ is the same with $V_{CE\_ON(Exp\_Ip)}$ as given in (3), it can be expected that bond-wire fatigue occurs.

$$\begin{aligned} \Delta R_{eq} > 0,\ V_{CE\_ON(Ip)} &= V_{CE\_ON(Exp\_Ip)} \\ &= V_{CE\_ON(Ref\_Ip)} + \Delta V_{CE\_ON(Ref\_Ip)} \end{aligned} \tag{3}$$

$V_{CE\_ON(Ref\_Ip)}$ is the reference V_{CE_ON} at the peak current obtained from the initial I-V characterization by the output currents as shown in Figure 4(b).
In the case of solder joint fatigue, $V_{CE\_ON(Ip)}$ increases due to the increase in thermal impedance. On the other hand, there is no variation in the $V_{CE\_ON(int)}$ since it is independent on the temperature change. From the initial I-V characterization by output currents, $V_{CE\_ON(Ref\_Ip)}$ can be obtained when I_P and T_A are known. If $V_{CE\_ON(Ip)}$ is higher than $V_{CE\_ON(Exp\_Ip)}$ and there is no variation in R_{eq} as given in (4), it can be expected that solder joint fatigue occurs.

$$\Delta R_{eq} = 0,\ V_{CE\_ON(Ip)} > V_{CE\_ON(Exp\_Ip)} \tag{4}$$

Further, the increment in T_j due to solder joint fatigue can also be obtained indirectly by the K-factor and difference between $V_{CE\_ON(Ip)}$ and $V_{CE\_ON(Exp\_Ip)}$.
When both failure modes occur at the same time, bond-wire fatigue leads to an increase in R_{eq} and the solder joint fatigue will make $V_{CE\_ON(Ip)}$ larger than $V_{CE\_ON(Exp\_Ip)}$. Thus, it can be expected that both failure modes occur if the condition given in (5) is satisfied

$$\Delta R_{eq} > 0,\ V_{CE\_ON(Ip)} > V_{CE\_ON(Exp\_Ip)} \tag{5}$$

Further, the contribution of each failure mode on the $V_{CE\_ON(Ip)}$ increase from the $V_{CE\_ON(Ref\_Ip)}$ can be determined.

4 Experimental Results

Experiments have been carried out in order to confirm the validity of the proposed method under the following condition; DC-link voltage (V_{DC}) = 350 V, output current (I) = 25 A_{peak}, output frequency (f_{out}) = 50 Hz, heat-sink temperature (T_H) = 40 ˚C.
In the 3-phase IGBT module, the low-side IGBT of phase-B is considered as target IGBT in the experiments as shown in Figure 1. Bond-wire fatigue is simulated by cutting the bond-wires of an open IGBT module. In the case of solder joint fatigue, it is emulated by changing heat-sink temperature (T_H). In the experiments, the initial charaterizations of the IGBT module are performed under different heat-sink temperatures T_Hs (40 ˚C, 50 ˚C and 55 ˚C). $V_{CE\_ON(int)}$, I_{int}, $V_{CE\_ON(Ref\_Ip)}$ and K-factor at 25 A are obtained as 1.062 V, 5 A, 1929 mV and 0.3 (˚C/mV), respectively. Finally, an average value of 100 measurements of each monitoring parameter is used in order to obtain accurate results.
V_{CE_ON} at different output currents and heat-sink temperatures are measured as shown in Figure 5 in order to verify the possibility to find intersection point from real-field data as mentioned in §2 (See Figure 4(c)).
It can be seen that the intersection point are found as 1.062 V at 5 A and it is the same with the value found from initial I-V characterization curves as shown in Figure 4(a). This result shows the possibility of the initial characterizations of IGBT modules from real-field data at the beginning of its installation.
Figure 6 shows the experimental result under both failure modes. In the experiment, $V_{CE\_ON(Ip)}$ is measured as 1927 mV, which is almost the same to $V_{CE\_ON(Ref\_Ip)}$, 1929 mV. Then, the bond-wire fatigue is simulated by cutting 2 bond-wires among 5 bond-wires. $V_{CE\_ON(int)}$ increases by 9 mV and thus ΔR_{eq} is 1.8 mΩ (9 mV/ 5 A).
From this, $\Delta V_{CE\_ON(Ref\_Ip)}$ is obtained as 45 mV based on (2) and finally $V_{CE\_ON(Exp\_Ip)}$ can be obtained as 1972 mV.

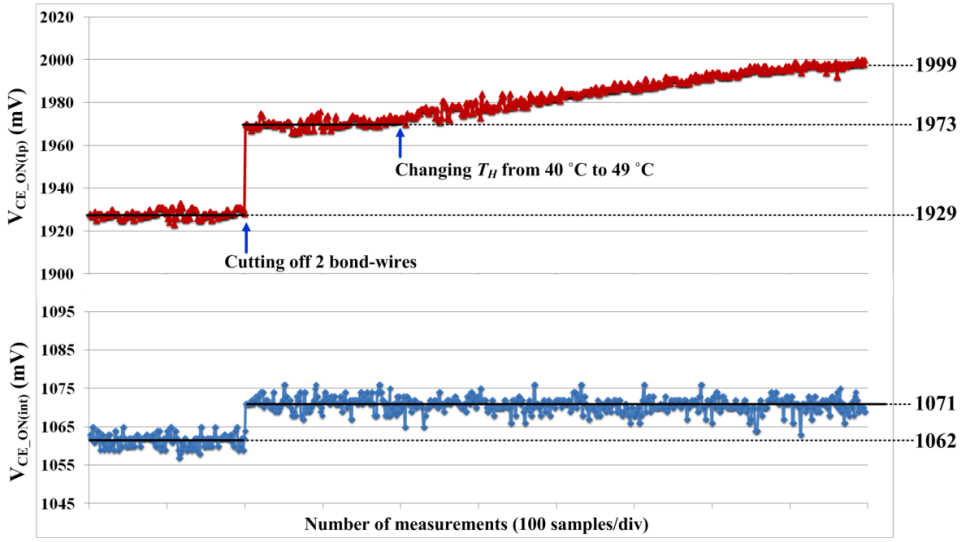

Figure 6 Experimental result under both bond-wire and solder joint fatigue when I = 25 A_{peak} where $V_{CE\_ON(Ip)}$ is V_{CE_ON} at peak current (25 A) and $V_{CE\_ON(int)}$ is V_{CE_ON} at intersection point (5 A).

TABLE I
SUMMARY OF EXPERIMENTAL RESULTS OF THE PROPOSED METHOD

Failure mode	T_H	$V_{CE\_ON(int)}$	$\Delta V_{CE\_ON(int)}$	ΔR_{eq}	$V_{CE\_ON(Ip)}$	$V_{CE\_ON(Exp\_Ip)}$	Error
Normal	40 ˚C	1062 mV	-	-	1929 mV	1927 mV	+2 mV
2 bond-wires cutting off	40 ˚C	1071 mV	9 mV	1.8 mΩ	1973 mV	1972 mV	+1 mV
2 bond-wire cutting off and solder joint fatigue	49 ˚C	1071 mV	9 mV	1.8 mΩ	1999 mV	2003 mV	-4 mV
3 bond-wires cutting off	40 ˚C	1081 mV	19 mV	3.8 mΩ	2025 mV	2022 mV	+3 mV

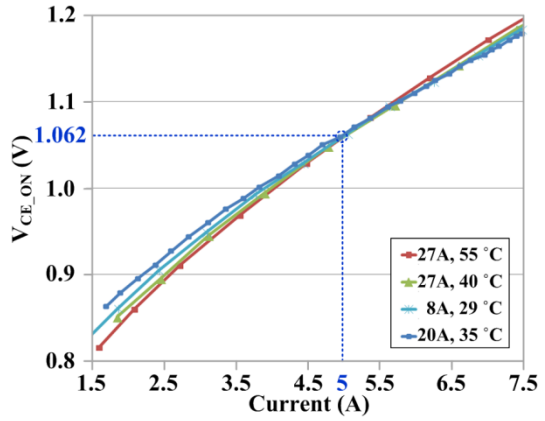

Figure 5 Characterization of an IGBT by outputs currents.

After cutting off 2 bond-wires, $V_{CE\_ON(Ip)}$ rises by 44 mV from 1929 mV to 1973 mV, which is almost the same to $V_{CE\_ON(Exp\_Ip)}$. This result satisfies the condition (3) for the detection of bond-wire fatigue. Then, T_H is changed from 40 ˚C to 49 ˚C in order to emulate solder joint fatigue. The $V_{CE\_ON(int)}$ is kept to 1071 mV, which is increased due to bond-wire fatigue. On the other hand, $V_{CE\_ON(Ip)}$ increases from 1973 mV to 1999 mV. $V_{CE\_ON(Ip)}$ is 26 mV larger than $V_{CE\_ON(Exp\_Ip)}$. From this, it can be estimated that there is about 8 ˚C increase in T_j and this value is almost similar with increased value in T_H which is 9 ˚C. Compared with initial value, $V_{CE\_ON(Ip)}$ increases by 70 mV and it is possible to determine that the 44 mV increase is due to bond-wire fatigue and the 26 mV increase is because of the solder joint fatigue.

Figure 7 shows the experimental results when 3 bond-wires are cut off. From the increased $V_{CE\_ON(int)}$, ΔR_{eq} and $\Delta V_{CE\_ON(Ref\_Ip)}$ are obtained as 3.8 mΩ and 95 mV, respectively. Thus, the $V_{CE\_ON(Exp\_Ip)}$ is 2022 mV. The measured $V_{CE\_ON(Ip)}$ is 2025 mV and this value is almost similar with $V_{CE\_ON(Exp\_Ip)}$. This result also meets eq. (3), which is the condition for determining the bond-wire fatigue.

The experimental results are summarized in TABLE I.

It is worth to note that the effect of the junction temperature on the resistance variation is not considered when equation (2) is applied for determining bond-wire fatigue. In order to investigate this effect, the worst case that 3 bond-wires out of 5 bond-wires are cut is considered. The junction temperature difference between at intesection point (5 A) and at peak current point (25 A) ($\Delta T_{j(int-Ip)}$) is assumed as 10 ˚C. Typically, this difference is not big because of fast output frequency. The bond-wires are aluminum and temperature coefficient of aluminum is 0.0039 $˚C^{-1}$ based on [13].

ISBN 978-3-8007-4540-1

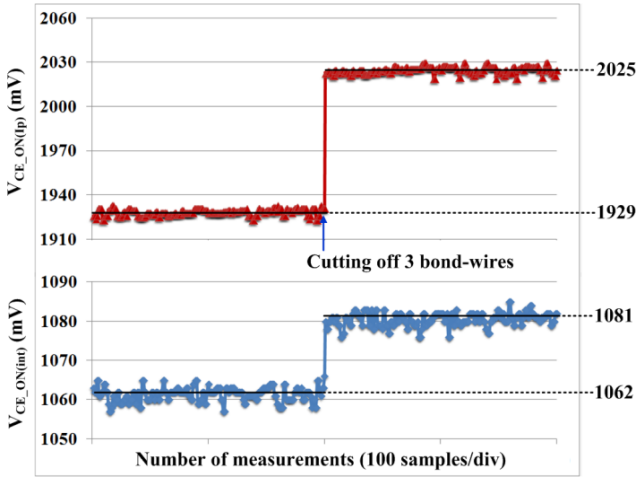

Figure 7 Experimental result when 3 bond-wires are cut where $V_{CE\_ON(Ip)}$ is V_{CE_ON} at peak current (25 A) and $V_{CE\_ON(int)}$ is V_{CE_ON} at intersection point (5 A).

When 3 bond-wires are cut, ΔR_{eq} is 3.8 mΩ and ΔR_{eq} at peak current will be changed as

$$\begin{aligned} \Delta R_{eq(Ip)} &= \Delta R_{eq} \cdot (1 + 0.0039\,°C^{-1} \times \Delta T_{j(int\text{-}Ip)}) \\ &= 3.8\,m\Omega + (3.8\,m\Omega \times 0.0039\,°C^{-1} \times 10\,°C) \\ &= 3.8\,m\Omega + 0.15\,m\Omega = 3.95\,m\Omega \end{aligned} \quad (6)$$

The increased ΔR_{eq} due to higher temperature at I_p than I_{int}, which is 0.15 mΩ results in 3.75 mV error (0.15 mΩ * 25 A) in $V_{CE\_ON(Ip)}$ at 25 A compared with $V_{CE\_ON(Exp\_Ip)}$ without considering this effect. Consequently, it leads to 1.1 ˚C error (3.75 mV * 0.3 (˚C/mV)). However, this error is small to determine that the solder joint fatigue also occurs. Therefore, this effect could be neglected in order to simplify the proposed method.

5 Conclusion

In this paper, a real-time condition monitoring method of IGBT module with failure mode separation has been proposed. This method can be achieved by monitoring V_{CE_ON} at the intersection point of I-V curves and the peak of output currents. The required characterizations of IGBT module can be obtained from the initial characterizations. It can also be obtained from real-field data thanks to the real-time V_{CE_ON} measurement circuit. The possibility of the initial characterizations from real-field data has been verified indirectly. The validity of the proposed method has been confirmed by the experiments in the laboratory with initial characterizations of the IGBT module. Further study needs to be performed such as the validation of the proposed method in real- field operation, initial characterization with real-field data and method to handle big real-field data effectively.

6 Literature

[1] Wang, H.: Lissere, M.: Blaabjerg, F: Toward Reliable Power Electronics: Challenges, Design Tools, and Opportunities, IEEE Industrial Electronics Magazine, Vol. 7, No. 2, June 2013, pp. 17-26

[2] Yang, Y.: Sangwongwanich, A.: Blaabjerg, F: Design for reliability of power electronics for grid-connected photovoltaic systems, CPSS Transactions on Power Electronics and Applications, Vol. 1, No. 1, Dec. 2016, pp. 92-103

[3] Yang, S.: Bryant, A.: Mawby, P.: Xiang, D.: Ran, L.: Tavner, P.: An Industry-Based Survey of Reliability in Power Electronic Converters, IEEE Transactions on Industry Applications, Vol. 47, No. 3, May/June 2011, pp. 1441-1451

[4] Volke, A.: Hornkamp, M.: IGBT Modules - Technologies, Driver and Application, Infineon Technologies AG, 2011, ISBN: 978-3-00-032076-7

[5] Choi, U. M.: Lee, J. S.: Blaabjerg, F.: Lee, K. B.: Open-Circuit Fault Diagnosis and Fault-Tolerant Control for a Grid-Connected NPC Inverter, IEEE Transactions on Power Electronics, Vol. 31, No. 10, Oct. 2016, pp. 7234-7247

[6] Choi, U. M.: Blaabjerg, F,: Lee, K. B.: Reliability Improvement of a T-Type Three-Level Inverter With Fault-Tolerant Control Strategy, IEEE Transactions on Power Electronics, Vol. 30, No. 5, May 2015, pp. 2660-2673

[7] Vernica, I.: Ma, K.: Blaabjerg, F,: Advanced derating strategy for extended lifetime of power Electronics in wind power applications, in Proc. of PEDG, Jun. 2016, pp. 1-8

[8] Yang, Y.: Wang. H, Blaabjerg, F.: Kerekes, T.: A Hybrid Power Control Concept for PV Inverter With Reduced Thermal Loading," IEEE Transactions on Power Electronics, Vol. 29, No. 12, Dec. 2014, pp. 6171-6275

[9] Ghimire, P.: Trintis, I.: Munk-Nielsen, S.: Rannestad, B.: On-state voltage drop based derating/uprating on a MW converter to improve reliability, Microelectronics Reliability, Vol. 58, Mar. 2016, pp. 90-94

[10] Ciappa, M: Selected failure mechanism of modern power modules, Microelectronics Reliability, Vol. 42, Nos. 4-5, Apr.-May 2002, pp. 653-667

[11] Choi, U. M.: Jorgensen, S.: Blaabjerg, F.: Advanced Accelerated Power Cycling Test for Reliability Investigation of Power Device Modules, Vol. 31, No. 12, Dec. 2016, pp. 8371-8386

[12] Choi, U. M.: Blaabjerg, F.: Munk-Nielsen, S.: Jorgensen, S.: Rannestad, B.: Reliability Improvement of Power Converters by Means of Condition Monitoring of IGBT Modules, IEEE Transactions on Power Electronics, Vol. 32, No. 10, Oct. 2017, pp. 7990-7997

[13] Choi, U. M.: Blaabjerg, F.: Iannuzzo, F. Jorgensen, S.: Junction Temperature Estimation Method for a 600V, 30A IGBT Module during Converter Operation, Microelectronics Reliability, Vol. 55, Nos. 9-10, Aug./Sep. 2016, pp. 2022-2026

